GEOPHYSICAL RESEARCH LETTERS, VOL. 20, NO. 5, PAGES 383-386, MARCH 5, 1993

PLUME STRUCTURES IN THE HARD-TURBULENT REGIME OF THREE-DIMENSIONAL INFINITE PRANDTL NUMBER CONVECTION

A. V. Malevsky and D. A. Yuen

Army High Performance Computing Research Center and Minnesota Supercomputer Institute, University of Minnesota

Abstract. Numerical simulations of three-dimensional infinite Prandtl number thermal convection with Rayleigh number (Ra) up to 10^8 are reported. Convection with Ra higher than 10^7 is characterized by the appearance of disconnected thermal plumes. The smaller plumes are detached by the currents produced by the larger plumes. The low wavenumber portion of a thermal power spectrum near the boundary layer becomes flat at high Ra, while the spectrum measured in the interior shows a positive slope for low wavenumbers. Differences are found in the thermal spectra between 2D and 3D models.

Introduction

Recently a new transition from soft to hard turbulence [Castaing et al., 1989] has been found in thermal convection of low Prandtl (Pr) number fluids. This transition, which is basically marked by the appearance of disconnected plumes, occurs at Ra between 10^7 and 10^8 and is relevant to thermal evolution of the Earth and other planets in their early stages [Yuen et al., 1993] and to convective processes in magma chambers. Thus far the numerical work on hard turbulence for infinite Pr fluids has been conducted in two-dimensional geometries [Hansen et al., 1990, Malevsky and Yuen, 1991]. Previous investigations of 3D infinite Pr convection [Houseman, 1988, Travis et al., 1990, Bercovici et al., 1989] have been restricted to the chaotic regime involving Ra of $O(10^6)$. With the arrival of a new generation of massively parallel supercomputers, such as CM-5, we can conduct large-scale 3D simulations of thermal convection in the hard turbulent regime, which means going to Ra well beyond 10^7.

3D Problem Formulation

We have used incompressible Boussinesq constant-viscosity fluid in modelling plumes developed in convection. Rayleigh number (Ra) is the sole control variable for this problem. We assume an impermeable top and bottom boundaries with free-slip conditions. Temperature is zero on the top and 1 on the bottom. Periodic boundary conditions are applied along the side boundaries. . For constant viscosity we need only poloidal stream function, Ψ:

$$\mathbf{u} = \nabla \times \nabla \times z\psi \qquad (1)$$

The horizontal boundaries of the computational domain are impermeable and stress-free. The boundary conditions for the stream-function and for the temperature are assumed to be periodic in x and y. We have introduced vorticity ω to solve two second-order equations for faster convergence of the conjugate gradient solver. The three-dimensional equations become:

Paper number 93GL00293
0094-8534/93/93GL-00293$03.00

$$\nabla^2\omega = -\mathrm{Ra}T$$

$$\nabla^2\psi = \omega$$

$$\frac{\partial T}{\partial t} + \mathbf{u}\cdot\nabla T = \nabla^2 T \qquad (2)$$

We have applied a method of characteristics to the nonlinear system (2). Stream-function and temperature were approximated by three-dimensional cubic splines. A predictor-corrector type scheme was used for the time-stepping. This scheme has been implemented on the Connection Machine [Malevsky et al., 1993]. We have verified the code against the case 17 from Travis et al. [1990], where a stable 2-D roll has been obtained in a box with the reflecting side boundaries and the aspect ratio $\sqrt{2}\times\sqrt{2}\times 1$ for $\mathrm{Ra}=10^5$. We calculated solution of the same problem with the periodic boundary conditions by doubling the horizontal dimensions of the box. Convection was started from the 2-D solution and ended in a stable two-roll configuration. The same characteristics-based scheme used for the time-dependent simulations has been used. The grid of 32x32x16 splines yielded the averaged value of $\mathrm{Nu}=9.64\pm0.4$, while $\mathrm{Nu}=9.75\pm0.11$ for the 48x48x20 grid. Both values differ by less than 5% from Nu=9.3 measured by Travis et al. [1990]. The accuracy of spatial approximation can also be judged by the decay of the wavenumber spectrum. The spectra of temperature and velocity anomalies exhibited a clear dissipative cutoff with two orders of magnitude. We have also checked the accuracy of the time-stepping in the time-dependent cases.

Results

We present results taken from 2D simulations with 128x64 bicubic splines on 32 processing nodes and for 3D model with up to 256x256x72 splines on 512 processing nodes of CM-5. Thermal plumes, which are responsible for thermal turbulence at infinite Pr, are produced at boundary layers. In the hard turbulent flow they may be detached later and travel in separate patches or diapirs. The convective interior is nearly isothermal, while the vicinity of the thermal boundary layer is unstable due to the adverse density stratification. This instability represents the main mechanism to produce the small scales in infinite Pr. The boundary layers are not uniform and can produce plumes of different sizes. This variety of scales reveals itself on the flat part of the spectrum of the temperature anomalies of hard turbulent convection [Yuen and Malevsky , 1992]. The flow field of convection with $\mathrm{Ra}=10^6$ consists mainly of plumes extended from one boundary layer to the other (Figure 1). These mushroom-like plumes are connected with each other through the shallow ridges on the top of a boundary layer. These ridges form a cellular structure on the surface. The spatial structure changes continuously. Convection with $\mathrm{Ra}=10^7$ is still dominated by the continuous plumes (Figure 2). Cells can still be observed on the surface, but their geometry is constantly evolving. The plumes are associated with the corners of the cells. The aspect-ratio of these cells becomes smaller with growing Ra.

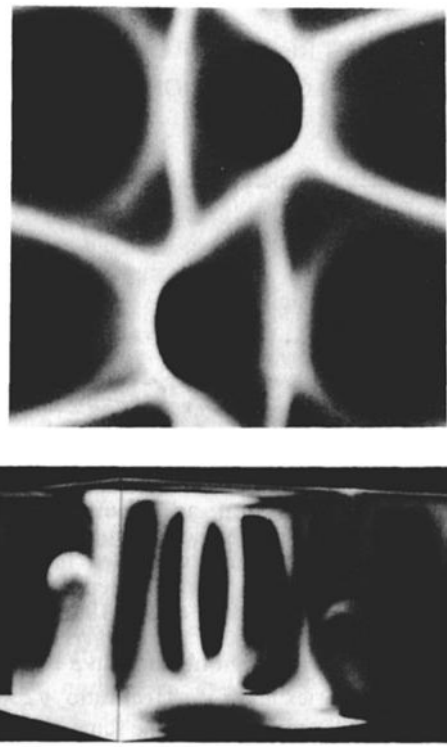

Fig.1. A snapshot of a temperature field of infinite Pr thermal convection with Ra=10^6 in a box with the aspect ratio $2\times2\times1$. Periodic boundary conditions have been imposed on the side boundaries and stress-free conditions have been maintained on the horizontal boundaries. Temperature ranges between 0 and 1. The isosurfaces of T=0.7 (lighter shade) and T=0.3 (darker shade) are shown on a side view (lower panel). A grid with 64x64x32 cubic splines has been employed. Each of the horisontal dimensions of this and subsequent figures of 3D convection was shortened by 30% for the purpose of visualization.

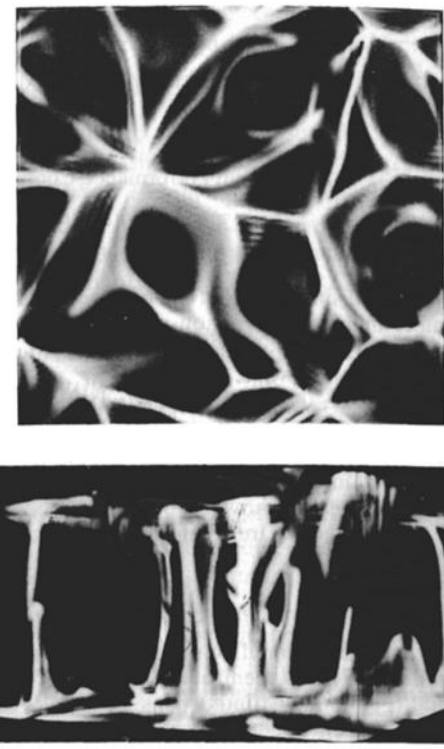

Fig. 2. Temperature fields of convection with Ra=10^7 in a box with the aspect ratio $2\sqrt{2}\times2\sqrt{2}\times1$. Temperature ranges between 0 and 1. Cellular structure of the hot boundary layer is shown on the bottom view (upper panel). The isosurfaces of T=0.7 and 0.3 are shown on a side view (lower panel). An isosurface of T=0.3 has the darker shade. A grid with 128x128x64 cubic splines has been employed. The ripples are artifacts from visualization.

Hansen et al. [1990] in 2D experiments demonstrated the increasing importance of the plume-plume collisions in the hard-turbulent regime. Collisions of the plumes with the same thermal signatures creates a cascade of energy from smaller to larger scales. On the other hand, collisions of the plumes with opposite signs represent a mechanism of energy transfer from the larger to the smaller scales, which is inherent only in the hard turbulent regime. The plumes are being cut into pieces as a result of the collisions. These flakes become later responsible for the smaller scales of motion. Collision of the plumes with the same thermal signatures may lead to the separation of a diapir. In Figure 3 we visualize the evolution of temperature field of convection with Ra=4x10^7 in a small portion of the domain. The large plume here attracts the rising small plume. Merging of the boundary layer instabilities with a "master" plume is an interesting phenomenon because of resultant amplification and can be observed in Figure 3. The stem of small plume is dragged by the circulation associated with the larger plume, while the "cap" of small plume detaches due to shear created by the larger plume. Later this cap travels separately from the stem. Interactive graphics software [Chin-Purcell, 1992] have allowed us to view the results of simulations as a time-dependent three-dimensional phenomenon, to observe the macroscopic patterns of the flow, to zoom into the details and to follow the evolution of the selected diapirs. This type of visualization is essential for investigating 3D hard turbulent convection. We have also made use of videos, which were very useful for understanding. Inspection of Figure 3 shows that the box on it has 32x32x64 tricubic splines which approximately correspond to 130x130x250 second-order finite-difference points, and all the spatial features have at least 2 spline intervals or 8 finite-difference points across.

Boundary layer instabilities usually originate on the ridges connecting these main plumes. We have also observed a collision of several well developed plumes rising from the corners of the cell when it collapses. The temperature field near a boundary layer is affected by the remnants of the plumes with opposite sign. Some remnant patches can stay there for a long time before being dissipated away by conduction process. Convection with Ra=10^8 is characterized by the appearance of disconnected plumes (Figure 4). These disconnected plumes at our highest Ra indicate that the flow is in hard turbulent state. The same phenomenon has been found in previous 2D simulations with reflecting boundary conditions [Hansen et al., 1990, Malevsky and Yuen, 1991]. A nonlinear interaction between the large-scale circulation with the boundary layer instabilities was responsible for early separation of the diapirs in these experiments. Large-scale circulation creates vortex sheets along the boundary layers. Shear associated with these vortices tears plumes apart from the boundary layer. Solomon and Gollub [1990] have observed that the additional shear applied along the horizontal boundary layers leads to the smaller plumes than those found in convection with no shear imposed. We can explain the mechanism for the plume separation as follows. Thinning of the stems of the plumes constitutes the first mechanism of separation. Plumes become thinner while they rise (or sink) due to buoyancy. Thinning of the plumes takes place continously with increasing Ra and does not indicate any distinct transition in the convective flow patterns. The second mechanism can only occur at high Ra. At high Ra plumes are

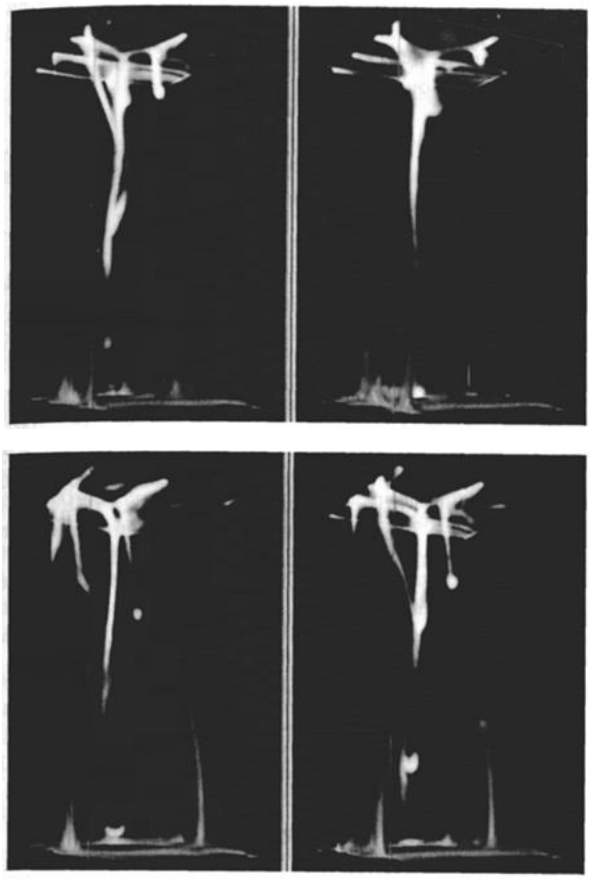

Fig.3. Evolution of a small part of convecting volume with Ra=4×10^7. Rising hot boundary layer instability is attracted by well developed master plume. The stem of small plume later collides with the master plume, while the "cap" detaches and travels as a separate diapir. The isosurfaces of T=0.7 and 0.3 are shown. Time step between the frames is 0.4×10^{-4}. Time is scaled with respect to thermal diffusion time. The size of the subdomain is 0.5x0.5x1.

torn off the boundary layer by the large scale circulation or by the nonlinear interactions between the plumes. Two-dimensional numerical experiments with reflecting boundary conditions revealed a persistent large scale circulation. We have not encountered a large-scale circulation in 2D and 3D models with the periodic boundary conditions imposed, but we have observed the plumes detached in the early stages by the flow associated with the larger, well-developed plumes.

The magnitudes of the different scales of motion are reflected by the wavenumber spectra of turbulent flow. Shape of a spectrum of convective turbulence is expected to change with depth, since the flow is anisotropic. We have calculated power spectrum of thermal variance $E_T(k)$ [Monin and Yaglom, 1975] at different depths. The spectrum has been averaged both in time and over the polar angle ϕ on the horizontal surface:

$$E_T(k_r,z)=\frac{1}{t}\int_0^t\int_0^{\frac{\pi}{2}}\theta^2(k_r,k_\phi,z,\tau)dk_\phi d\tau \qquad (3)$$

where (k_r, k_ϕ, z) is a cylindrical coordinate decomposition of the wavenumber **k** and θ is the temperature fluctuation with respect to the horizontally averaged temperature profile. In 2D simulations with the reflecting boundary conditions the low-wavenumber part of the spectrum becomes flat with the transition to hard turbulence [Yuen and Malevsky, 1992]. In

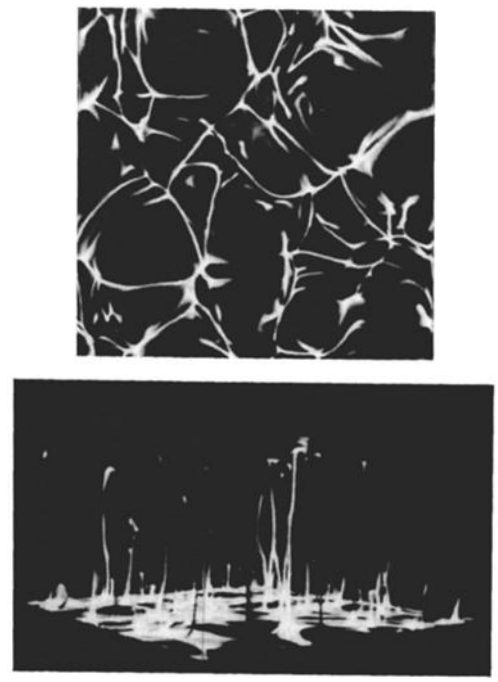

Fig.4. Temperature fields of convection with Ra=10^8 in a box with the aspect ratio $2\sqrt{2}\times2\sqrt{2}\times1$. Temperature ranges between 0 and 1. Cellular structure of the hot boundary layer is shown on the bottom view (upper panel). The isosurfaces of T=0.7 and 0.3 are shown on a side view (lower panel). An isosurface of T=0.3 has the darker shade. A grid with 256x256x72 cubic splines has been employed.

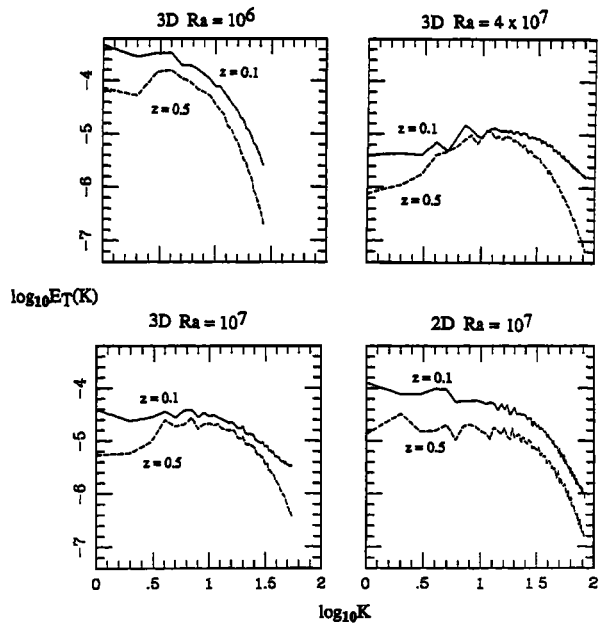

Fig.5. Wavenumber power spectra of temperature fluctuations of infinite Pr thermal convection measured in 3D and 2D simulations. The spectra have been averaged both in time and over a horizontal plane. The spectra at two depths, z=0.1 and 0.5 are given.

3D simulations with the periodic boundary conditions the spectrum measured near the boundary layer is flat at high Ra as well, but the spectra in the interior of convecting volume have a very different shape (Figure 5). Power spectrum of temperature fluctuations in the middle of the layer exhibits a

positive slope for low wavenumbers. The maximum indicates a characteristic size of a temperature anomaly and hints to an energy and thermal perturbation input caused by the plumes with smaller scales [Grossmann and Lohse, 1992]. This maximum shifts to a higher wavenumber for larger Ra. In high wavenumber dissipative subrange the spectra decay faster than k^{-3}.

We have also conducted 2D simulations of convection in a box of the aspect ratio $2\sqrt{2}$ with the periodic boundary condition for comparing the spectra obtained in 2D and 3D models. Unlike the 3D simulations, 2D models do not yield a positive slope of the power spectra of temperature fluctuations. The spectra here are always flat at low wavenumber (Figure 5). The flat part of the spectrum is followed by the high wavenumber exponential dissipative cutoff. The portion of the spectrum with a positive slope is a 3D effect. There is a close correspondence between 2D and 3D spectra measured near the boundary layer. This suggests that the initiation of the boundary layer instabilities may be a 2D effect, while the subsequent evolution of the plumes differs in 2D and 3D. The boundary layer instabilities originate at the ridges connecting the main plumes (Figure 4), but they later grow as prominent 3D structures. The spectra of convective turbulence obtained in numerical simulations are also influenced by the boundary conditions. In 2D simulations [Malevsky et al., 1992] at $Ra=10^8$ we found that flows with the periodic boundary conditions yielded a negative slope of kinetic energy spectrum with -3, while for the free-slip boundaries the slope was around -2. Stress-free or reflecting side boundaries create the vertical boundary layers, which significantly affect the patterns of the flow field. The time-averaged Nusselt number (Nu) of 37 has been measured for both 2D and 3D simulations with $Ra=10^7$.

Discussion

We have studied plume structures in 3D convection for infinite Pr in the hard turbulent regime. Boundary layers in 3D convection are not uniform and produce thermal anomalies with different sizes, which show up as the flat part of the thermal spectra. Boundary layer instabilities represent the main mechanism to produce the small scales. The collisions of hot and cold plumes represent another mechanism of energy transfer from the larger to the smaller scales, found in hard turbulence. The onset of disconnected plumes occurs at nearly the same Ra of $O(10^7)$ in 2D and 3D. This finding is encouraging for the application of the hard turbulent concept to mantle convection [Yuen et al., 1993].

Acknowledgments. This research was supported in part by the Innovative Research Program of NASA. A. Malevsky has been a recipient of Army High Performance Computing Research Center postdoctoral fellowship under contract number DAAL03-89-C-0038. We thank P. Morin for his creative help in the visualization of three-dimensional convection and Detlef Lohse for constructive remarks.

References

Bercovici, D., G. Schubert and G. Glatzmaier, Three-dimensional spherical models of convection in the Earth's mantle, Science, 244, 950-955, 1989.

Castaing, B., G. Gunaratne, G. Heslot, F. Kadanoff, A. Libchaber, S. Thomae, X.Z. Wu, S. Zaleski and G. Zanetti, Scaling of hard thermal turbulence, J. Fluid Mech, 204, 1-30, 1989.

Chin-Purcell, K., All about BOB: a tool for browsing 3D data sets, AHPCRC preprint 92-141, University of Minnesota, Minneapolis, 1992.

Grossmann, S. and D. Lohse, Scaling in hard turbulent Rayleigh-Benard flow, Phys. Rev., A 46, 903-917, 1992.

Hansen, U. , D.A. Yuen and S.E. Kroening, Transition to hard turbulence in thermal convection at infinite Prandtl number, Phys. Fluids, A2(12), 2157-2163, 1990.

Houseman, G.A., The dependence of convection planform on mode of heating, Nature, 332, 346-349, 1988.

Malevsky, A.V. and D.A. Yuen, Characteristics-based methods applied to infinite Prandtl number thermal convection in the hard turbulent regime, Phys. Fluids, A3(9), 2105-2115, 1991.

Malevsky, A.V., D.A. Yuen and K.E. Jordan, Method of characteristics applied to two- and three-dimensional thermal convection on the Connection Machine, to appear in the Proceedings of 7th IMACS Conference on Computer Methods for PDE, 1993.

Monin, A. and A.M. Yaglom, Statistical Fluid Mechanics, vol. 2., MIT Press, Cambridge, MA, 1975.

Solomon, T.H. and J.P. Gollub, Sheared boundary layers in turbulent Rayleigh-Benard convection, Phys. Rev. Lett. 64, 2382-2385, 1990.

Travis, B., P. Olson and G. Schubert, The transition from two-dimensional to three-dimensional planforms in infinite Prandtl number thermal convection, J. Fluid Mech. 216, 71-91, 1990.

Yuen, D.A., U. Hansen, W. Zhao, A.P. Vincent and A.V. Malevsky, Hard turbulent thermal convection and thermal evolution of the mantle, J. Geophys. Res., in press, 1993.

Yuen, D.A. and A.V. Malevsky, Strongly chaotic Newtonian and non-Newtonian mantle convection, in Chaotic Processes in Geological Sciences, ed. by D.A. Yuen, pp.71-88, Springer-Verlag, Berlin, 1992.

A.V. Malevsky and D.A. Yuen, Minnesota Supercomputer Institute, 1200 Washington Ave., South Minneapolis, MN 55415.

(Received October 20, 1992;
accepted December 29, 1992)